A poxvirus-encoded pyrin domain protein interacts with ASC-1 to inhibit host inflammatory and apoptotic responses to infection

Johnston, James B.; Barrett, John W.; Nazarian, Steven H.; Goodwin, Megan; Ricuttio, Dan; Wang, Gen; McFadden, Grant

Publisher's version / Version de l'éditeur:
https://doi.org/10.1016/j.immuni.2005.10.003
Immunity (Cambridge, Mass.), 23, December 6, pp. 587-598, 2005

Immunity, Vol. 23, 587–598, December, 2005, Copyright ©2005 by Elsevier Inc. DOI 10.1016/j.immuni.2005.10.003

A Poxvirus-Encoded Pyrin Domain Protein Interacts with ASC-1 to Inhibit Host Inflammatory and Apoptotic Responses to Infection

James B. Johnston,[1,3] John W. Barrett,[1] Steven H. Nazarian,[1,2] Megan Goodwin,[2] Dan Ricuttio,[2] Gen Wang,[1,3] and Grant McFadden[1,2,*]
[1] BioTherapeutics Research Group
Robarts Research Institute
1400 Western Road
London, Ontario N6G 2V4
Canada
[2] Department of Microbiology and Immunology
University of Western Ontario
London, Ontario N6A 5C1
Canada

Summary

Proinflammatory caspases play an essential role in innate immune responses to infection by regulating the cleavage and activation of proinflammatory cytokines. Activation of these enzymes requires the assembly of an intracellular molecular platform, termed the inflammasome, which is comprised of members of the pyrin domain (PYD)-containing superfamily of apoptosis and inflammation-regulatory proteins. We report here the identification and characterization of a poxvirus-encoded PYD-containing protein that interacts with the ASC-1 component of the inflammasome and inhibits caspase-1 activation and the processing of IL-1β and IL-18 induced by diverse stimuli. Knockout viruses that do not express this protein are unable to productively infect monocytes and lymphocytes due to an abortive phenotype and are markedly attenuated in susceptible hosts due to decreased virus dissemination and enhanced inflammatory responses at sites of infection. Thus, modulation of inflammasome function constitutes an important immunomodulatory strategy employed by poxviruses to circumvent host antiviral responses.

Introduction

In any given host-pathogen interaction, a fine and delicate balance exists between the ability of the host to clear the pathogen and the ability of the pathogen to evade or suppress host defenses. One consequence of this coevolution is that pathogens encode highly developed and specific proteins to counteract the versatile innate and adaptive host immune responses to infection. Poxviruses, in particular, encode an expansive repertoire of immunomodulatory proteins (Seet et al., 2003). Although many of these proteins are dispensable for replication in culture, they are often critical to productive infection of an immunocompetent host. Principal among these viral proteins are those that target innate processes instrumental to limiting and resolving infections, such as apoptotic and inflammatory response pathways. So effective are these strategies that several poxvirus-encoded immunomodulators have been proposed for use as therapeutic agents in the treatment of inflammatory diseases (Lucas and McFadden, 2004).

Myxoma virus (MV) is a rabbit-specific poxvirus that is the causative agent of myxomatosis, a generalized disseminated infection characterized by the formation of an extensive fulminating lesion at the primary site of infection and a viremia that spreads the infection through the host lymphoreticular system to secondary organs and tissues (Fenner and Ratcliffe, 1965). Death of the host rapidly follows MV infection due, in part, to supervening bacterial infections that accompany suppression of the host immune system. This immunosuppression reflects the concerted activity of the many immunomodulatory proteins encoded by MV (Barrett et al., 2001). Among these proteins is the product of the M13L gene, a putative immunomodulator possessing the PYRIN domain (PYD) that is the defining feature of the PYD superfamily of apoptosis and inflammatory regulators (Fairbrother et al., 2001; Stehlik and Reed, 2004).

The PYD is structurally similar to the death-domain-fold (Fairbrother et al., 2001), a protein-protein interaction motif found in death domains (DD), death effector domains (DED), and caspase activation recruitment domains (CARD). Like these domains, the PYD likely mediates homotypic protein-protein interactions between components of signaling pathways involved in the regulation of apoptosis, NF-κB activation, and proinflammatory cytokine production (Fairbrother et al., 2001). Although the functions of many PYD proteins are still being determined, approximately 20 members have been identified in humans (Reed et al., 2003). Moreover, their potential to regulate apoptotic and inflammatory signaling pathways is supported by evidence implicating several PYD family members in the etiologies of hereditary autoinflammatory diseases that share the symptom of persistent systemic inflammation, including familial Mediterranean fever (FMF), familial cold autoinflammatory syndrome (FCAS), Muckle-Wells syndrome, and chronic infantile neurological cutaneous and articular syndrome (Centola et al., 1998; Hoffman et al., 2001; Hull et al., 2003; McDermott and Aksentijevich, 2002).

For some PYD family members, such as the pyrin-only protein (POP)-1, the PYD is the sole functional motif within the protein. Many others, however, possess effector domains in addition to the N-terminal PYD, such as the CARD of ASC-1 (apoptosis-associated speck-like protein containing CARD-1) or the NACHT domain of cryopyrin (Reed et al., 2003). Recently, a model for procaspase-1 activation has been proposed whereby inflammatory stimuli promote the formation of the inflammasome, a molecular scaffold comprised of ASC-1, NALP-1, and caspases-1 and -5 (Martinon et al., 2002). In this model, PYD-mediated interactions between ASC-1 and NALP-1 expose distinct CARD motifs within each protein that recruit and activate procaspase-1, leading to the production of interleukin (IL)-1β and IL-18. This process is modulated by other PYD family

*Correspondence: mcfadden@robarts.ca
[3] Present address: Institute for Nutrisciences and Health, National Research Council of Canada, 93 Mount Edward Road, Charlottetown, Prince Edward Island C1A 5T1, Canada.

members, including pyrin, cryopyrin, and POP-1, which interact with the inflammasome via their PYD domains to promote or inhibit inflammasome activity (Richards et al., 2001; Stehlik et al., 2003; Yu et al., 2005).

We report here the identification and characterization of the M13L gene product, M13L-PYD, a poxvirus-encoded protein that contains an N-terminal PYD domain. Deletion of M13L attenuates MV virulence in rabbits, producing a phenotype in which myxomatosis does not develop and the infection is rapidly resolved in the absence of mortality despite an enhanced acute inflammatory response to infection. This loss of virulence correlates with decreased virus spread and dissemination from primary sites of infection due to an abortive infection of monocytes and lymphocytes. We further demonstrate that M13L-PYD colocalizes and interacts with a cellular PYD protein, ASC-1, to modulate caspase-1 activity and processing of IL-1β and IL-18. Thus, M13L-PYD is a virus-encoded member of the PYD superfamily and a component of a potentially novel poxvirus anti-inflammatory strategy.

Results

The MV M13L Gene Encodes a PYD Protein

The product of the MV M13L open reading frame (ORF) was initially identified as a 13 kDa, nonsecreted, early viral protein that shared similarity with the p200 family of IFN-inducible (IFI) proteins (Cameron et al., 1999). Based on the lack of signal sequences for either secretion or nuclear localization, it was classified as a cytosolic protein of indeterminate function. More recent analyses have revealed an 81 residue domain at the amino terminus (N-term) of the M13L product that shares 69% amino acid similarity (42% identity) with the PYD (Figure 1A). Designated M13L-PYD, the protein lacked other identifiable functional domains and appeared to be a virus-encoded member of the PYD superfamily. Moreover, PYD-containing proteins were identified in the genomes of other poxviruses, including the closely related Leporipoxvirus, Shope fibroma virus (SFV, gp013L), the Yatapoxvirus, Yaba-like disease virus (YLDV, ORF18L), and the Suipoxvirus, swinepox virus (SPV, ORF014L) (Figure 1B). Thus, poxvirus PYD proteins were conserved among diverse poxvirus genera.

Deletion of M13L Attenuates MV and Impedes Virus Dissemination In Vivo

To determine the role of M13L-PYD in MV pathogenesis, recombinant M13L knockout (KO) viruses were constructed by inserting a green fluorescence protein (GFP) cassette under the control of a synthetic early/late poxvirus promoter either within (vMyxgfpΔPYD) or downstream of (vMyxgfpΔCterm) the PYD (Figure 1C). To ensure the absence of adverse recombination events, revertant viruses (vMyxrevPYD) were generated by restoring the intact M13L ORF. A recombinant virus in which GFP was inserted into a noncoding site (vMyxgfp) served as wild-type (wt) control. New Zealand White (NZW) rabbits were then infected by subdermal flank injection of each virus, and disease progression was evaluated daily over a 2 week period. Clinical results are summarized in Figure 2A and described in detail in Table 1. Rabbits infected with wt or revertant viruses exhibited clinical symptoms consistent with myxomatosis, and two-thirds of the animals in each group (4/6) were euthanized within 10 days postinfection (PI) (Figure 2A). In contrast, infection with vMyxgfpΔPYD was nonlethal, and all animals (4/4) survived after exhibiting comparatively mild symptoms that were resolved by day 9 PI (Figure 2A). The second KO virus, vMyxgfpΔCterm, was also attenuated relative to wt virus, but infections were slower to resolve and half of the animals (2/4) were euthanized by day 13 PI (Figure 2A).

The characteristic clinical feature of myxomatosis is the formation of necrotic lesions, termed myxomas, at both the initial (primary lesion) and distal (secondary lesions) sites of infection (Fenner and Ratcliffe, 1965). Dissemination of MV to secondary sites likely involves infected leukocytes traveling via the lymphatic system. Consistent with vigorous virus spread, secondary lesions were abundant on the noses, ears, and eyelids of rabbits infected with wt or revertant viruses (Table 1). GFP-positive cells, from which infectious virus could be isolated, were also prevalent in peripheral blood collected from these animals (Figure 2B). Similarly, secondary lesions were evident in all animals infected with vMyxgfpΔCterm (Table 1) concurrent with circulating infected leukocytes (Figure 2B). In comparison, small satellite and secondary lesions that rapidly resolved were found in only half of the vMyxgfpΔPYD-infected rabbits (Table 1), while GFP-positive cells were detected sporadically in peripheral blood (Figure 2B). Thus, loss of M13L-PYD function appeared to impair dissemination of MV by infected peripheral leukocytes.

Differences were also observed at the site of inoculation. Primary lesions progressed more rapidly in rabbits infected with vMyxgfpΔPYD compared to the other viruses, becoming raised and inflamed by day five PI (Table 1). Active virus replication was indicated by the presence of strong GFP fluorescence, but these lesions did not spread and rapidly ulcerated and regressed. In contrast, the primary lesions induced by wt and revertant viruses were slower to develop, continued to spread, and became necrotic (Table 1). Primary lesions in vMyxgfpΔCterm-infected rabbits developed at a rate comparable to wt and revertant viruses, but regressed more quickly once recovery began (Table 1). RT-PCR analysis revealed that proinflammatory markers, such as IL-1β, IL-6, and macrophage chemoattractant protein, were barely detectable in the primary lesions induced by wt and revertant viruses (Figure 2C). These cytokines were markedly upregulated in primary lesions tissue from vMyxgfpΔPYD-infected rabbits, however, suggesting that acute inflammatory responses at the primary site of infection were elevated in the absence of M13L-PYD.

The M13L KO Virus Is Attenuated due to Impaired Infection of Leukocytes

To further investigate the possibility that dissemination of vMyxgfpΔPYD was impaired by the inability to productively infect leukocytes, growth curves were generated for KO and control viruses after infection of rabbit RK13 fibroblasts and RL5 lymphocytes. All viruses replicated equally well in RK13 cells, forming foci indicative of virus spread and reaching similar maximum titers (Figure 3A). However, vMyxgfpΔPYD was attenuated in RL5 cells and replicated to lower titers than the other

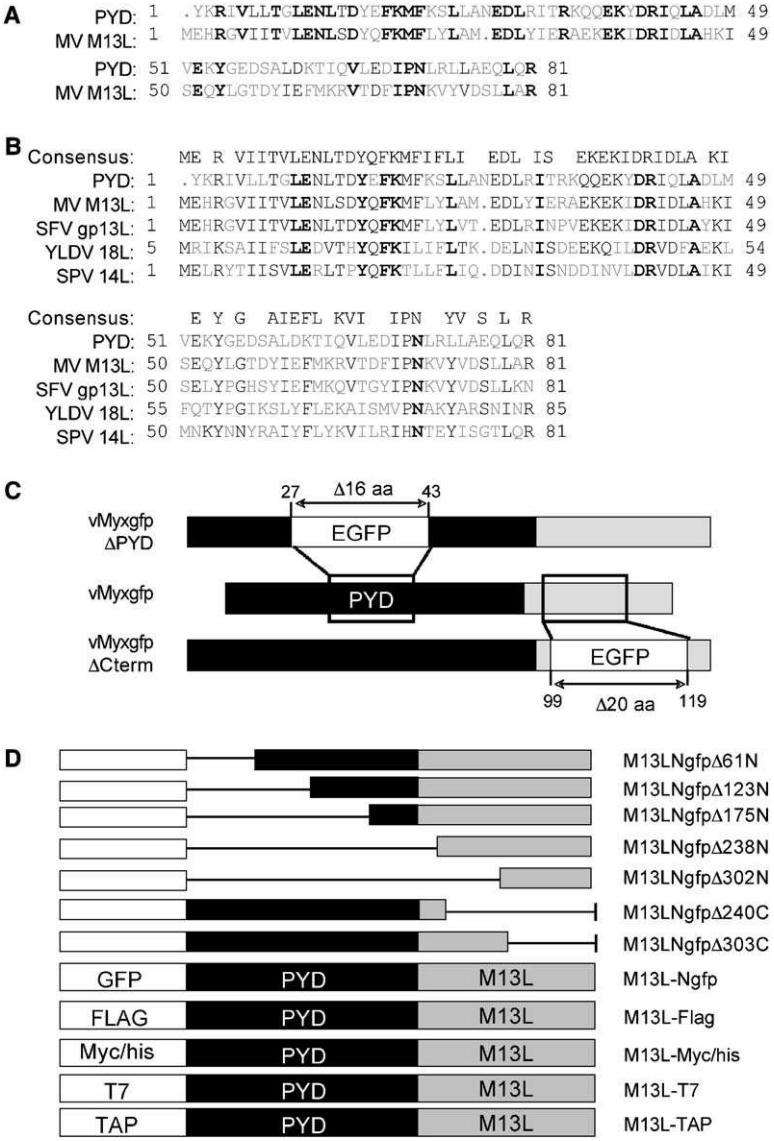

Figure 1. Bioinformatic Analyses and Manipulation of the M13L ORF

(A) CLUSTAL alignment of the 81 residue N-terminal PYD from M13L and the NCBI sequence for the PYD domain (PAAD/DAPIN, pfam02758.11). Residues are color-coded as having identity (bold black), similarity (black), or no similarity (gray).

(B) Partial alignment of PYD proteins from MV and other poxviruses, including SFV (NP051902), YLDV (NP073403), and SPV (NP570174). The consensus sequence for this alignment is shown.

(C) M13L KO viruses were constructed by targeted disruption of the M13L ORF and insertion of a GFP cassette (EGFP) driven by a synthetic early/late viral promoter. The GFP cassette was inserted either within the PYD starting at aa 27 (vMyxgfpΔPYD) or downstream of the PYD starting at aa 99 (vMyxgfpΔCterm).

(D) Summary of the epitope tags used to construct M13L-PYD fusion proteins. Deletion mutants of M13L-Ngfp were generated by progressive truncation of sequences from either the amino (N) or the carboxyl (C) terminus at the indicated residues by PCR primer walking.

viruses (Figure 3B). Similar results were observed using primary rabbit peripheral blood lymphocytes (PBL) and monocytes (PBM). Titers obtained from cells infected with vMyxgfp and vMyxrevPYD were much higher than those obtained with vMyxgfpΔPYD (Figure 3C). Thus, deletion of M13L-PYD was associated with a decreased ability to productively infect cells of lymphoid and myeloid lineages.

Expression and Subcellular Localization of M13L-PYD

PYD proteins associated with inflammasome formation (Masumoto et al., 1999) and their regulators (Mansfield et al., 2001) are typically expressed within the cytosol; therefore, we next investigated the subcellular localization of M13L-PYD. Fluorescence microscopy of human 293T fibroblasts transiently transfected with a plasmid expressing GFP alone revealed fluorescence that was diffuse and not associated with specific subcellular structures (Figure 4A). In contrast, GFP-tagged M13L-PYD (M13L-Ngfp) initially exhibited a discrete perinuclear distribution after transfection in 293T cells, but was dispersed throughout the cytosol as aggregates or punctate bodies by 72 hr (Figure 4A). A similar expression pattern was observed in transfected human THP-1 monocytes (Figure 4A) and in rabbit fibroblasts in the context of infection (Figure 4A). This pattern did not reflect the GFP tag since M13L-PYD-Myc/his fusion proteins also localized to discrete cytosolic bodies (data not shown), and an N-term GFP tag has been shown not to affect the localization or function of other PYD proteins (Mansfield et al., 2001; Masumoto et al., 2001). A comparable perinuclear expression profile has been described for pyrin and was erroneously reported to represent localization to the Golgi complex (Chen et al., 2000). Similarly, M13L-Ngfp expressed in 293T cells did not colocalize with fluorescent markers specific for either the Golgi (Figure 4B) or the endoplasmic reticulum (ER). A fluorescent endolysosomal marker did colocalize with perinuclear M13L-Ngfp, but not with the late-forming cytosolic aggregates of M13L-PYD (Figure 4B).

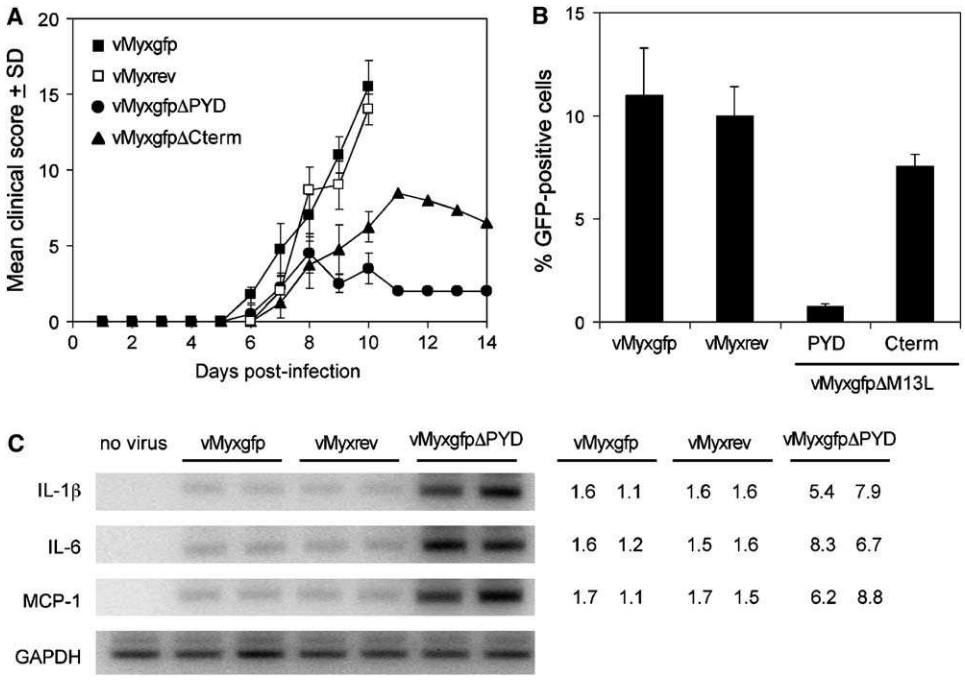

Figure 2. Disruption of the M13L ORF Attenuates MV

Adult NZW rabbits were infected in each flank by intradermal injection of wt MV (vMyxgfp), M13L KO viruses (vMyxgfpΔPYD, vMyxgfpΔCterm), or a revertant virus (vMyxrevPYD).

(A) Summary of the mean clinical scores (+SD) assigned to each group after daily rankings according to a graduated scale. Larger values indicate poorer clinical outcomes due to greater disease severity. Clinical scores are not available after day 10 PI for rabbits infected with vMyxgfp or vMyxrevPYD due to poor survival rates.

(B) Fluorescence microscopy detection of MV-infected cells in PBMC isolated at day 7 PI from representative animals in each infected group. Values are expressed as a percentage of total cells isolated and represent the average number of GFP-positive cells in four samples ± SD.

(C) Primary lesion tissue was harvested at day 5 PI from two rabbits in each group, and the expression of host molecules upregulated during inflammation was assessed by semiquantitative RT-PCR via primers specific for rabbit IL-1β, IL-6, and MCP-1. Dermal tissue from an uninfected rabbit served as a control (no virus). Band intensities were determined by densitometry and values are indicated in arbitrary units following correction for the intensity of GAPDH.

The subcellular distribution of PYD proteins is determined largely by their PYD even when other functional domains are encoded (Mansfield et al., 2001; Richards et al., 2001). Thus, M13L GFP fusion proteins were generated by targeted deletion of sequences both within and outside of the PYD (Figure 1D) and expressed in 293T cells by transfection. As illustrated with M13LΔ61D, from which the first 22 amino acids of the PYD had been removed, disruption of the M13L PYD resulted in a loss of both the early perinuclear distribution (data not shown) and the late cytosolic dispersion (Figure 4C). In contrast, deletions outside of the PYD did not alter this profile significantly, and even a fusion protein comprised of the M13L PYD alone (M13LΔ240C) continued to localize in cytosolic bodies (Figure 4C). Taken together, these findings indicated that M13L-PYD followed an expression profile similar to known cytosolic PYD proteins that was dependent on an intact PYD.

ASC-1 Is a Binding Partner of M13L-PYD

PYD family members that interact with ASC-1 and modulate its activity have been shown to colocalize with ASC-1 in perinuclear and cytosolic bodies in a PYD-dependent manner (Masumoto et al., 1999; Richards et al., 2001). Given the expression profile of M13L-PYD, we next assessed whether M13L-PYD also colocalized with ASC-1. Following expression in 293T cells, M13L-Ngfp and Myc/his-tagged ASC-1 were found to colocalize within both the perinuclear bodies at 48 hr (Figure 4D, insets) and the cytosolic aggregates at 72 hr (Figure 4D). Subsequent studies suggested that this colocalization reflected a specific interaction between ASC-1 and M13L-PYD. Binding of ASC-1 to M13L was assessed by coimmunoprecipitation and Western blot in 293T cells cotransfected with plasmids expressing M13L-PYD and ASC-1 tagged with Flag or Myc/his epitopes. Consistent with an interaction between these proteins, Myc/his-tagged ASC-1 was detected in elutants following immunoprecipitation of M13L-Flag, but not in cells transfected with a control vector that did not express M13L-PYD (Figure 4E). This finding was supported by the reciprocal experiment in which Myc/his-tagged M13L-PYD was detected by Western blot in elutants following ASC-Flag pull-downs (Figure 4E).

An in vitro binding assay was then used to determine whether this interaction occurred under biologically relevant conditions. Lysates from 293T cells transfected with M13L-PYD tagged with the tandem affinity purification (TAP) epitope were incubated with lysates from activated THP-1 cells, and binding partners were isolated using the TAP method (Wang et al., 2004). Following separation by SDS-PAGE, silver staining revealed a prominent band at a molecular weight of 22 kDa that

Table 1. Pathogenicity of vMyxgfp, vMyxrevPYD, vMyxgfpΔPYD, and vMyxgfpΔCterm

Day PI	vMyxgfp	vMyxrevPYD[a]	vMyxgfpΔPYD	vMyxgfpΔCterm
3	primary (1 cm)	primary (1 cm)	primary (1 cm)	primary (1 cm)
5	primary raised (2.5 cm)	primary raised (2 cm)	primary raised (3.5 cm); inflamed; crown flattened	primary raised (1.6 cm)
		no satellites		some satellites
		decreased food and water intake		
7	primary larger (4.0 cm)	primary larger (3.0 cm)	healing	primary larger (2.7 cm)
	numerous satellites (3–15)	numerous satellites (4–10)	ulcerating, cavitating primary	small satellites
	secondary lesions on nose, ears, eyelids	secondary lesions on nose and eyelids	small satellites and secondary lesions on 2 rabbits	small secondary lesions on ears
	swollen head			ano-genital inflammation
	ano-genital inflammation			
9	primary large, inflamed	primary large (4 cm)	healing	primary larger but ulcerating
	satellites too numerous to discern	numerous satellites >10	primary and secondary lesions regressing	secondary lesions on lip
	ears and head swollen; fur ruffled	secondary lesions on ears, nose, and eyelids (2–10)	animals recovering	small secondary lesions on ears and lips
	numerous secondary lesions	discharge from eyes		animals recovering
	swollen eyelids, multiple lesions, discharge	nose and head swollen, fur ruffled		
	ano-genital inflammation	ano-genital inflammation		
14	33% survival[b]	33% survival	100% survival	50% survival

[a] Revertant virus constructed in the vMyxgfpΔPYD background.
[b] Indicates proportion of animals that were not sufficiently moribund at day 14 PI to warrant euthanasia.

was subsequently confirmed to be ASC-1 by mass spectrometric analysis (Figure 4F). A similar interaction between M13L-PYD and other members of the PYD superfamily has not been observed by mass spectrometry when M13L-PYD is used as bait. Under the experimental conditions used, only ASC-1 has been detected in elutants. Taken together, these findings indicated that M13L-PYD interacted with ASC-1 and establish the potential for the viral protein to impact on the regulation of inflammation and apoptosis after infection.

Expression of M13L-PYD Inhibits Caspase-1 Activation in Monocytes

The phenotype of the M13L-PYD KO virus implied a role for the protein in suppressing host apoptotic or inflammatory responses to infection. Since caspase-1 participates in both pathways and is tightly regulated by ASC-1 and other components of the inflammasome, we next investigated the impact of M13L-PYD on caspase-1 activity. Untransfected THP-1 cells and cells expressing M13L-Ngfp, M13L-NgfpΔ61N, or GFP alone were subjected to mechanical disruption or incubated in the presence or absence of LPS, and caspase-1 activation was assessed by Western blot detection of the cleavage of procaspase-1 to its active form. THP-1 cells were selected because they constitutively express PYD proteins that are activated by mechanical disruption and LPS treatment (Martinon et al., 2002) and because M13L-PYD can be expressed in these cells by high-efficiency transfection (Figure 4A) or by direct infection with MV (unpublished data). The cleaved, activated isoform of caspase-1 was readily detectable in untransfected cells or cells expressing GFP alone after mechanical disruption or stimulation with LPS, but only minimal caspase-1 cleavage was evident in THP-1 cells expressing M13L-PYD (Figure 5A). As demonstrated after expression of M13L-NgfpΔ61N, disruption of the M13L-PYD restored inhibition of caspase-1 activation to wt levels (Figure 5A). These findings were confirmed using a colorimetric caspase-1 activity assay in which expression of intact, but not truncated, M13L-PYD reduced caspase-1 activity by approximately 50% under the same experimental conditions (Figure 5B). We next determined whether expression of M13L-PYD could also inhibit the biological consequences of caspase-1 activation by detecting processing of the proinflammatory cytokine, IL-1β. Western blot analyses confirmed that LPS treatment or mechanical disruption induced abundant IL-1β processing in untransfected cells and cells expressing GFP or M13L-NgfpΔ61N, but that expression of M13L-Ngfp inhibited IL-1β processing after either stimulus (Figure 5C). Similarly, levels of secreted IL-1β in CM from M13L-Ngfp-transfected cells were decreased by approximately 30% compared to levels in control cultures when a quantitative sandwich ELISA was used (Figure 5D).

The impact of M13L-PYD on caspase activation in the context of poxvirus infection was also investigated. Infection of THP-1 cells with vMyxgfpΔPYD was itself sufficient to induce caspase-1 processing that was largely absent in uninfected cells or cells infected with wt virus (Figure 6A). However, it should be noted that Western blot analysis revealed additional bands following detection of caspase-1 in MV-infected cells that were not present in transiently transfected cells. Whether these observations are nonspecific or represent additional processing of caspase-1 induced by active infection is unclear. Of interest, no differences were observed in the activation of caspase-3, a primary component of the intrinsic apoptosis pathway, after infection with either wt

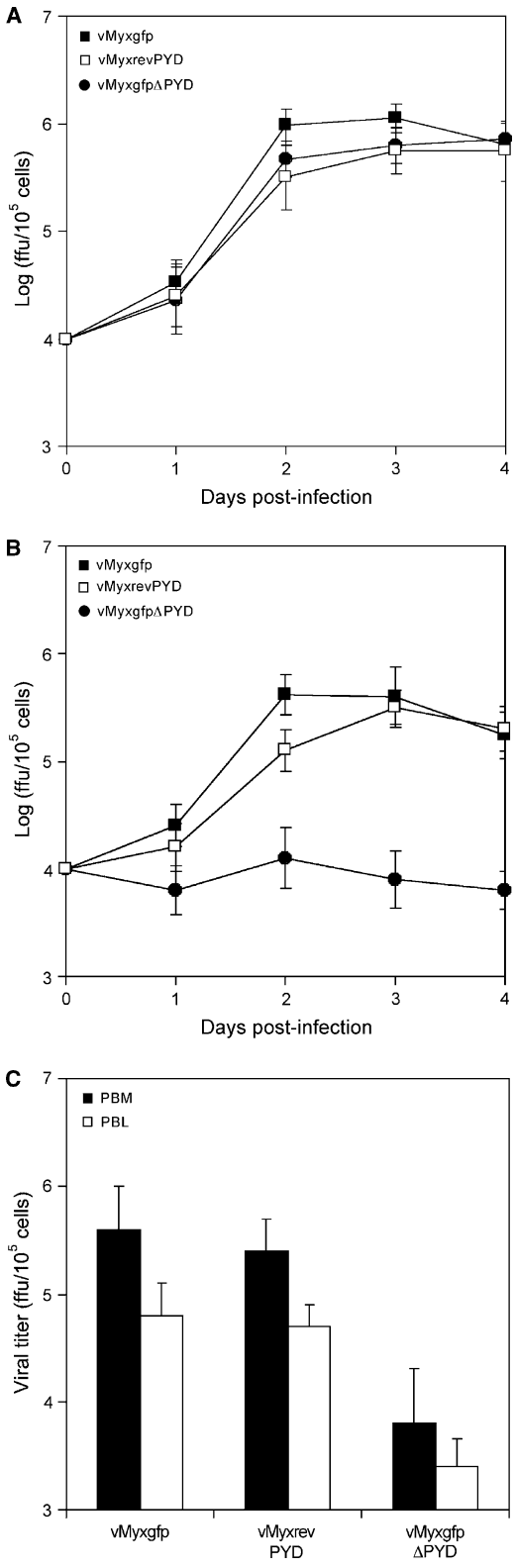

Figure 3. Deletion of the M13L ORF Restricts MV Replication in Leukocytes

Multistep growth curves from rabbit RK13 fibroblasts (A) and RL5 lymphocytes (B) after infection at moi = 0.01 and titration of progeny virus on BGMK cells. Values represent log (mean titer) from triplicate wells ± SD.

(C) Primary rabbit PBM and PBL were infected at moi = 1 and viral titers were measured at 48 hr PI.

MV or the M13L-PYD KO virus (Figure 6A). Compared to mock-infected cultures, only minimal caspase-3 processing was observed in cells infected with either virus. The inhibitory effect of M13L-PYD was not limited to events induced by infection since caspase-1 activation was also decreased in THP-1 cells that were infected with vMyxgfp prior to stimulation with LPS or mechanical disruption (Figure 6B). In contrast, cells infected with vMyxgfpΔPYD exhibited higher levels of caspase-1 activity in response to either stimulus (Figure 6B), indicating that expression of M13L-PYD in infected cells also altered responses to exogenous stimuli.

Consistent with the results obtained in Figure 5, activation of caspase-1 was associated with increased processing of IL-1β. Levels of secreted, active IL-1β were elevated in CM from THP-1 cells infected with wt or KO virus relative to mock-infected cells (Figure 6C). However, only minimal increases were observed in vMyxgfp-infected cells, whereas IL-1β concentrations in CM from cells infected with vMyxgfpΔPYD were increased by more than 3-fold during the 48 hr time course. Similar results were observed with IL-18, another proinflammatory cytokine that undergoes processing by caspase-1 (Akita et al., 1997). Although levels of secreted, active IL-18 were increased in CM from THP-1 cultures infected with either wt or KO virus relative to mock-infected cells at 12 hr PI, IL-18 was 2.3-fold more abundant in THP-1 cells infected with vMyxgfpΔPYD (Figure 6C). Moreover, IL-18 levels in vMyxgfp-infected THP-1 cultures decreased below that of mock-infected cells as infection progressed, while IL-18 remained elevated in KO virus-infected cultures. Thus, expression of M13L-PYD during MV infection was associated with increased caspase-1 activation and concurrent processing and secretion of proinflammatory cytokines.

Discussion

Poxviruses employ a diverse array of proteins to downregulate innate or acquired host immune responses by targeting such processes as apoptosis; the production of interferons, chemokines, and inflammatory cytokines; and the activity of cytotoxic T cells, natural killer cells, complement, and antibody (Seet et al., 2003). The obvious sequence similarity between some poxvirus genes and the cDNA versions of cellular counterparts suggests that they are the product of ancestral capture, recombination, and reassortment events that occurred during coevolution of the virus and its vertebrate hosts (McLysaght et al., 2003). Consistent with that hypothesis, we have described the initial characterization of a new class of poxvirus immunomodulatory proteins typified by the product of the MV M13L ORF, M13L-PYD. Structurally and functionally, M13L-PYD closely resembles members of the PYD superfamily of proteins that regulate apoptotic and inflammatory signaling pathways in myeloid cells (Bertin and DiStefano, 2000; Gumucio et al., 2002). Here, we report the ability of M13L-PYD to interfere with the host inflammasome complex and thus block this aspect of the cellular proinflammatory responses to the virus infection.

The case for membership in this family is multifold. From a structural viewpoint, M13L-PYD possesses the

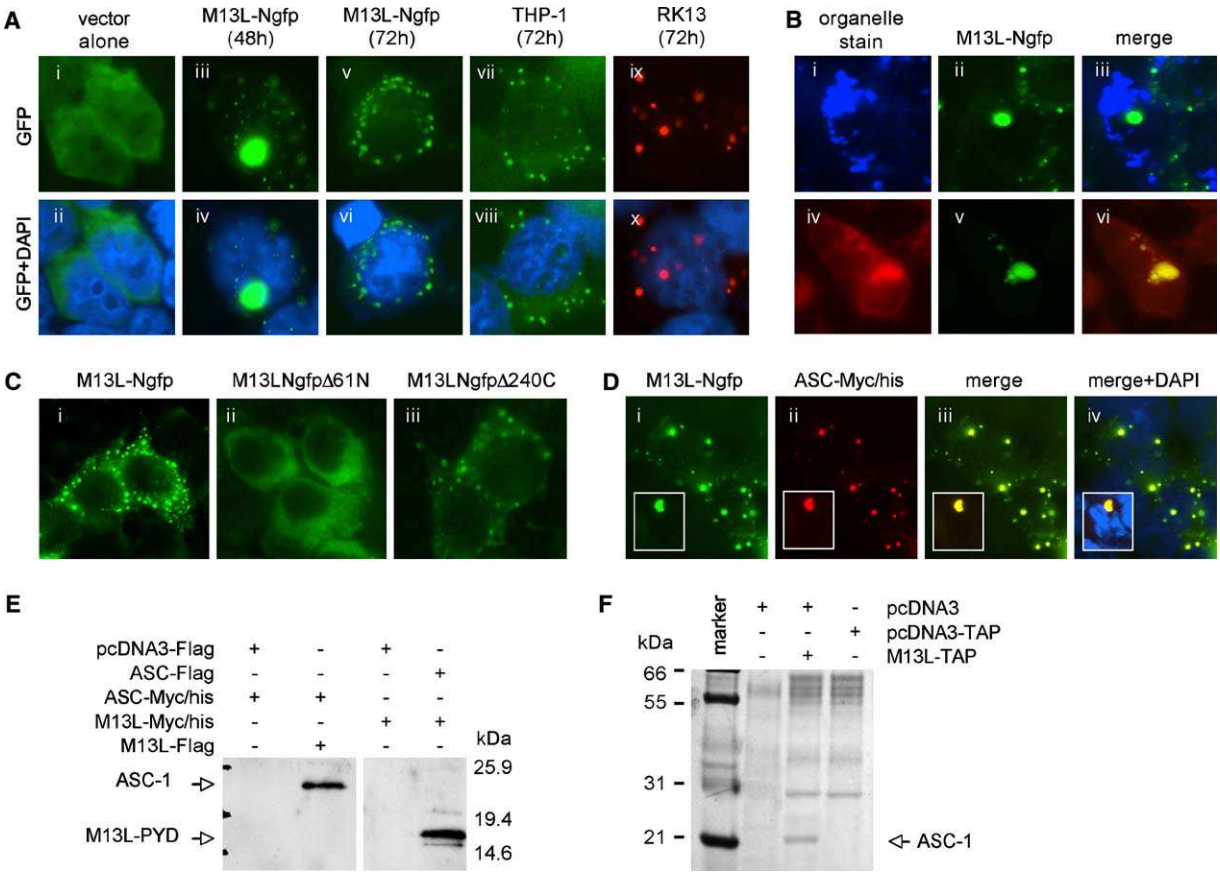

Figure 4. Expression and Subcellular Localization of M13L-PYD

(A) M13L-Ngfp was expressed by transfection in human 293T fibroblasts (i–vi) and differentiated THP-1 monocytes (vii and viii), and localization was assessed at 48 or 72 hr by fluorescence microscopy. Nuclei are shown in blue after DAPI counterstaining. T7-tagged M13L-PYD under the control of an early/late VV promoter was expressed in rabbit RK13 cells that were infected with vMyxgfpΔPYD (ix and x). Expression of M13L-PYD was detected by indirect immunofluorescence with antibody against the T7 epitope and a TRITC-conjugated secondary antibody (original magnification, 640×).

(B) Subcellular localization of M13L-Ngfp in 293T cells was assessed at 48 hr by fluorescent stains specific for the Golgi complex (Golgitracker, blue, i–iii) or lysosomes (lysotracker, red, iv–vi) (original magnification, 640×).

(C) Localization of representative GFP fusion proteins generated by successive truncation of M13L-PYD within (M13LNgfpΔ61N, ii) or outside of (M13LNgfpΔ240C, iii) the PYD. Proteins were expressed in 293T and compared to full-length M13L-Ngfp (i) (original magnification, 400×).

(D) Colocalization of M13L-Ngfp (i) and Myc/his-tagged ASC-1 (ii) was assessed 48 hr (insets) and 72 hr after cotransfection in 293T cells. ASC-1 expression was detected by indirect immunofluorescence with TRITC-conjugated secondary antibody to detect the Myc epitope.

(E) Representative Western blots showing the interaction between M13L-PYD and human ASC-1 expressed in 293T cells by cotransfection. Left: Flag-tagged M13L was immunoprecipitated by antibody specific for the Flag epitope (IP, anti-Flag), and bound Myc/his-tagged ASC-1 was detected by immunoblot with antibody against the Myc epitope (IB, anti-Myc) in elutants from cells transfected with plasmid expressing M13L-Flag but not the Flag epitope alone (pcDNA3-Flag). Right: The reciprocal experiment with Flag-tagged ASC-1 and Myc/his-tagged M13L.

(F) Lysates from 293T cells transfected with TAP-tagged M13L were incubated with lysates from activated THP-1 cells and bound proteins isolated with the TAP method. A representative silver-stained gel following separation of bound proteins by SDS-PAGE is shown with arrows indicating a prominent band with a molecular weight of the 22 kDa that was determined to be ASC-1. This band was not evident when lysates obtained from 293T cells transfected with empty plasmid (pcDNA3) or plasmid expressing the TAP epitope alone (pcDNA3-TAP) were analyzed.

N-term PYD that defines members of the PYD superfamily (Fairbrother et al., 2001). In fact, like PYD proteins such as POP-1, the M13L gene product consists almost entirely of a single PYD and encodes no other functional domain or motif. Moreover, the M13L PYD shares a high degree of similarity with the classical PYD sequence and it is a critical determinant of the properties of M13L-PYD. From a functional perspective, M13L-PYD exhibited the capacity to modulate caspase-1 activation and inflammatory cytokine processing pathways in myeloid cells that have previously been shown to be regulated by PYD family members, such as ASC-1 (Srinivasula et al., 2002). As with other PYD proteins, the PYD of M13L was implicated as a potential determinant of this function. Consistent with the role of the PYD as a homotypic protein-protein interaction motif, M13L-PYD colocalized in the cytosol with ASC-1 and was found to interact with this protein in binding assays. Taken together, these findings constitute strong evidence that M13L-PYD is in fact a functional viral PYD protein.

Poxvirus immunomodulatory proteins can be divided by function into three strategic classes: virostealth proteins, viromimetics (virokines and viroreceptors), and virotransducers (Seet et al., 2003). M13L-PYD appears to be a member of this latter group, which act intracellularly to micromanipulate host-cell signal transduction

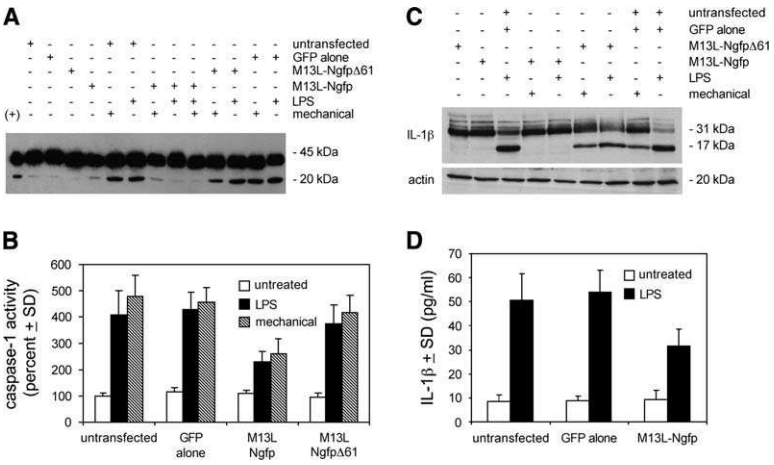

Figure 5. Expression of M13L-PYD Inhibits Caspase-1 Activation and IL-1β Processing

Full-length M13L-Ngfp or truncated M13L-NgfpΔ61N were expressed in differentiated human THP-1 cells by transient transfection. (A and C) Caspase-1 and IL-1β activation was induced by mechanical disruption of membrane integrity or stimulation with LPS (600 μg/ml for 6 hr). Activation of caspase-1 (A) and IL-1β (C) was assessed by Western blot detection of the active, cleaved isoform of each enzyme. Detection of the housekeeping gene, actin, ensured equal loading.

(B) Caspase-1 activity in parallel cultures was quantified by spectrophotometric detection of *p*NA-YVAD cleavage and changes were expressed as a percentage (±SD) of values obtained for untreated controls (100%).

(D) IL-1β levels in conditioned media from LPS-treated cells were quantified by sandwich ELISA and were expressed as pg of cytokine/ml of CM ± SD.

machinery and disconnect innate antiviral pathways from their biological effect. MV encodes several virotransducers that target apoptosis and caspase activity, including the antiapoptotic serine protease inhibitor (serpin), Serp-2, and the apoptotic regulators encoded by the MV M11L, M-T4, and M-T5 genes (Everett and McFadden, 1999). Of these, only the MV Serp-2 protein has been shown to weakly inhibit caspase-1 activity and modulate inflammatory and apoptotic responses in lymphoid cells (Messud-Petit et al., 1998). However, unlike M13L-PYD in this study, Serp2 has limited effect on the activity of human caspase-1 (Messud-Petit et al., 1998) and is unlikely to have significantly influenced the results reported here. Thus, M13L-PYD may represent the primary modulator of caspase-1 activation encoded by MV.

When comparing the properties of M13L-PYD with those of PYD proteins that function as regulators of the activity of other PYD proteins, such as pyrin, numerous parallels are evident. M13L-PYD exhibits a high degree of similarity with pyrin, particularly within the first 50 residues of the PYD. Like pyrin (Mansfield et al., 2001; Richards et al., 2001), M13L-PYD exhibits a distinctive cytosolic and punctate perinuclear distribution that was dependent on sequences within the PYD. For pyrin, this pattern also reflected colocalization with ASC-1 (Richards et al., 2001). Thus, at first blush it may seem surprising that expression of M13L-PYD is associated with decreased caspase-1 activation, whereas the interaction between pyrin and ASC-1 is a proinflammatory event (Yu et al., 2005). Since the only functional domain encoded by M13L is the PYD, it is conceivable that M13L-PYD binds to ASC-1 via a homotypic interaction mediated by the PYD and inhibits its activation similar to POP-1 (Stehlik et al., 2003). However, M13L-PYD shares little sequence similarity with POP-1 (data not shown). Alternatively, M13L-PYD may bind to ASC-1 and acts as a competitive inhibitor of pyrin to prevent ASC-1 activation. This model is consistent with the mechanism of action of other poxvirus immunomodulatory proteins that are homologs of cellular proteins (Seet et al., 2003). Although we have yet to find evidence of a potential interaction between M13L-PYD and other PYD family members, the high degree of similarity between the PYDs of M13L and IFI proteins that are expressed in the cytosol, such as myeloid nuclear differentiation antigen (MNDA) (Asefa et al., 2004), may indicate alternate functions for M13L-PYD.

The sequences of more than two dozen poxvirus genomes have been determined and immunomodulatory proteins targeting all facets of innate and adaptive immune responses have been reported (Seet et al., 2003). In fact, so diverse are these genes that a single immunomodulatory protein that is common to all poxviruses has yet to be identified. However, genes predicted to encode PYD proteins that closely align with M13L-PYD are also present in the genomes of poxviruses from other *Leporipoxviridae*, as well as representatives from the *Suipoxviridae* (Afonso et al., 2002) and the *Yatapoxviridae* (Lee et al., 2001). Phylogenetic analyses have demonstrated that, together with the *Capripoxviridae*, these three genera cluster to form the largest subgrouping of Chordopoxviruses (Gubser et al., 2004), suggesting a common evolutionary ancestor that may have initially acquired a host PYD protein. However, no gene analogous to M13L has been identified in the genomes of the capripoxvirus species that have been sequenced to date (Tulman et al., 2001, 2002), possibly indicating an earlier evolutionary divergence from other viruses in this group. Of particular interest is the fact that orthopoxviruses, such as vaccinia virus (VV) (Calderara et al., 2001), and the molluscipoxvirus, molluscum contagiosum (Xiang and Moss, 2003), encode secreted proteins that act as molecular scavengers to bind and sequester IL-1β, whereas comparable orthologs are absent in members of the *Capripoxvirus*, *Leporipoxvirus*, *Suipoxvirus*, and *Yatapoxvirus* genera (Barry and McFadden, 1997). Thus, poxvirus-encoded PYD proteins capable of disrupting the intracellular signaling pathways leading to IL-1β processing and secretion may serve a similar role.

Advances in the field of viral immunomodulation continue to be made with increasing frequency, providing important clues about the selective pressures that drive the coevolution of virus and host. Moreover, greater understanding of the mechanisms by which poxviruses

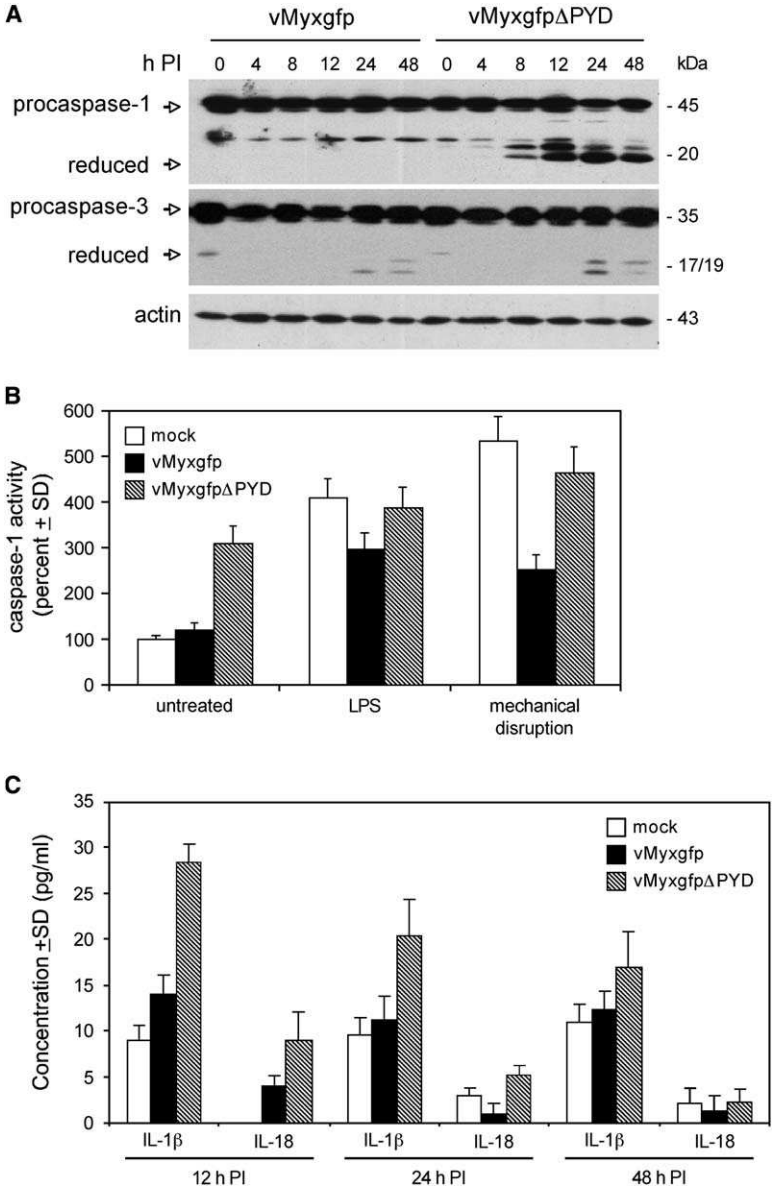

Figure 6. Deletion of M13L-PYD Results in Increased Caspase-1 Activity

Differentiated THP-1 cells were mock-infected or infected with vMyxgfp and vMyxgfpΔPYD, and cells and CM were harvested at the indicated times PI.

(A) Expression of caspase-1 and caspase-3 was assessed by Western blot.

(B) Caspase-1 activity induced in mock- or MV-infected THP-1 cells by LPS stimulation (600 μg/ml for 6 hr) or mechanical disruption was measured via a *p*NA-YVAD cleavage assay and changes were expressed as a percentage (±SD) of values obtained for mock-infected controls (100%).

(C) Levels of secreted IL-1β and IL-18 were determined by ELISA and expressed as pg of cytokine/ml of CM ± SD.

modulate key components of the immune system has increased the potential for viral immunomodulatory proteins to be used as therapeutic agents (Lucas and McFadden, 2004). Deregulated IL-1β production and chronic inflammation are hallmarks of many autoimmune diseases that present both systemically and within the central nervous system, including rheumatoid arthritis and multiple sclerosis (Kinne et al., 2000; Minagar et al., 2002). Thus, poxvirus immunomodulatory proteins that target monocyte activity and regulation of IL-1β may have the potential to be exploited in the design of novel anti-inflammatory therapies for the treatment of these diseases.

Experimental Procedures

Cell Culture

BGMK, RK13, and 293T cells were cultured in DMEM (GIBCO-BRL) completed with 10% fetal bovine serum (FBS) and antibiotics. THP-1 monocytes and rabbit RL5 lymphocytes were cultured in complete RPMI 1640 medium (GIBCO-BRL). For differentiation, THP-1 cells were stimulated for 24 hr with 50 ng/ml phorbol-12-myristate-13-acetate (PMA, Sigma). PBMC used in infection studies were obtained from healthy NZW rabbits and isolated by density-gradient centrifugation, as described previously (Johnston and Power, 1999). Blood-derived PBM were separated from PBL by adherence on polystyrene flasks for 1 hr and maintained in complete RPMI. Nonadherent PBL were collected and cultured in complete RPMI supplemented with recombinant IL-2 (100 IU/ml, Sigma).

Viruses

Recombinant and KO viruses were constructed in a MV (strain Lausanne) background and propagated and titrated using the methods described previously (Opgenorth et al., 1992). Wild-type vMyxgfp contained a GFP cassette driven by a synthetic VV early/late promoter that was inserted between ORFs M135R and M136R (Johnston et al., 2003). Two KO viruses deficient for M13L-PYD expression were similarly constructed by selectively deleting specific sequences within the M13L ORF and inserting a GFP cassette by homologous recombination: vMyxgfpΔPYD, for which nucleotides 14852 to 14902 within the M13L-PYD were deleted, and vMyxgfpΔCterm, for which nucleotides 14633 to 14690 near the C terminus of M13L

were removed (Figure 1C). Disruption of the M13L ORF was confirmed by PCR and gel shift analyses. To ensure that the phenotype of each KO virus did not reflect adverse mutations introduced into other genes during recombination, a revertant virus was constructed (vMyxrevPYD) to restore the intact M13L ORF. Infections were performed and growth curves constructed as previously described (Johnston et al., 2005)

Animal Studies

NZW rabbits were housed in level 2 containment facilities at the University of Western Ontario Animal Care Facility according to the guidelines of the Canadian Council on Animal Care. Experiments were conducted on two separate dates using different preparations of each virus. Injections were performed intradermally in each thigh using 1000 focus forming units (ffu) of vMyxgfp (n = 9), vMyxrevPYD (n = 4), vMyxgfpΔPYD (n = 7), or vMyxgfpΔCterm (n = 4) per site. Two rabbits injected with PBS served as controls. Disease progression was monitored daily for symptoms consistent with Myxomatosis (Fenner and Ratcliffe, 1965) and scored on a graduated scale according to disease severity by animal care technicians unaware of the status of the animal. A clinical score between 0 (complete absence of disease) and 20 (moribund) was assigned to each rabbit, with moribund animals sacrificed using euthanyl administered intravenously after anesthesia. Animals from each group were also sacrificed at 4, 7, and 10 days PI, and a complete postmortem examination was performed. Tissue, including the primary and secondary lesions, spleen, and lymph nodes, was collected and divided into two samples that were either snap frozen in liquid nitrogen for isolation of RNA and protein or embedded in paraffin for analysis by immunohistochemistry. To detect circulating MV-infected cells, PBMC were isolated from blood collected by intravenous puncture at day 3 and 7 PI and immediately visualized by fluorescence microscopy to detect the GFP expression indicative of MV infection.

Fusion Proteins and Epitope-Specific Antibodies

The complete M13L ORF, and M13L variants in which specific regions of the M13L ORF were selectively deleted, were PCR amplified from genomic viral DNA and subcloned into expression vectors using restriction sites introduced by the PCR primers (Figure 1D). Constructs included fusion proteins expressing TAP (cDNA3.6-TAP, Wang et al. [2004]), Myc/his (pcDNA3.1myc-his, Invitrogen), and GFP (phrGFP-N, Stratagene) epitopes. Flag and T7 tags were introduced during amplification of M13L with PCR primers containing sequences encoding the epitope. Plasmid encoding untagged human ASC-1 was kindly provided by J. Reed (The Burnham Institute, La Jolla, CA) (Stehlik et al., 2002). Flag and Myc/his epitope-tagged ASC-1 were generated by subcloning into the appropriate vector. The identities of all clones were confirmed by sequence analysis, and expression of fusion proteins was confirmed by fluorescence microscopy or Western analyses via mouse monoclonal antibodies specific for Myc (Invitrogen), T7 (Novagen), Flag (Sigma), or GFP (Clontech) epitopes. Gel shift analysis was used to confirm that the fluorescence observed represented a GFP fusion product. A rabbit peroxidase-anti-peroxidase antiserum (anti-PAP; Sigma) recognizing the protein A sequence was utilized for detecting the TAP tag.

Subcellular Localization of M13L-PYD

Human 293T cells were grown to 90% confluence and transiently transfected with plasmids encoding full-length or truncated M13L fusion proteins using Lipofectamine 2000 reagent (Invitrogen) in accordance with the manufacturer's instruction. After 24 hr, transfected cells were harvested, adhered to poly-L-lysine-coated coverslips, and cultured as indicated. PMA-differentiated THP-1 cells were adhered to coverslips at 50% confluence and transfected using ExGen 500 Reagent (Fermentas, Inc.). Untransfected cells and cells transfected with the appropriate plasmid lacking exogenous sequences (vector alone) served as controls. At 48 hr and 72 hr post-transfection, cells were mounted on glass slides in Prolong Antifade medium (Molecular Probes) and assessed by fluorescence microscopy. To detect subcellular localization, transfected cells were counterstained with fluorescent markers (Molecular Probes) targeting the Golgi complex (BODIPY FL C_5-ceramide, 1:100), endoplasmic reticulum (ER-Tracker Blue-White DPX, 1:750), mitochondria (MitoFluor Red 589, 1:5000), actin (Texas red-X phalloidin, 1:20), lysosomes (LysoTracker Red DND-99, 1:13000), or the nucleus (DAPI, 1:330).

To determine M13L-PYD localization in the context of MV infection, RK13 cells were initially transfected with pSC65 plasmid encoding M13L-T7 under the control of the VV early/late promoter. Transfected cells were infected after 24 hr with vMyxgfpΔPYD at moi = 1 and cultured for an additional 24 or 48 hr. M13L expression was assessed by indirect immunofluorescence by the use of monoclonal antibody specific for the T7 epitope (1:100) and a TRITC-conjugated goat-anti-mouse secondary antibody (1:500, Jackson ImmunoResearch). Isotype control antibodies were used to ensure the lack of nonspecific antibody binding.

Immunoprecipitation and TAP Purification

293T cells were cotransfected with plasmid encoding FLAG-tagged M13L or Myc/his-tagged ASC-1 and cultured for 72 hr. Transfected cells were lysed in CellLytic-M reagent (Sigma) containing protease inhibitors and cleared lysates incubated overnight with anti-FLAG agarose beads (Sigma). Beads were pelleted by centrifugation, washed twice, and incubated at 65ºC for 10 min in SDS-PAGE sample buffer containing 100 mM DTT. The eluted complexes were resolved by SDS-PAGE and then analyzed by immunoblotting with antibodies against the Myc/his epitope. The reciprocal experiment was conducted in the same manner with M13L tagged with the Myc/his epitope and FLAG-tagged ASC-1. For TAP isolations, 293T cells transfected with M13L conjugated to either the TAP or Myc/his epitope were lysed in 2% CHAPS buffer containing protease inhibitors, and the lysates were cleared by centrifugation. Lysates from approximately 10^7 THP-1 cells were prepared by passage through a 22 gauge needle as described, combined with the 293T cell lysates and incubated overnight at 4ºC. The M13L-TAP fusion protein and associated proteins were then isolated using the TAP method described previously (Wang et al., 2004), concentrated to an appropriate volume, and resolved by SDS-PAGE. Separated proteins were visualized by silver staining (Bio-Rad).

Immunoblot Analyses

Protein levels in cleared cell lysates were quantified with a protein assay kit (Bio-Rad), and Western blot analyses were performed as previously described (Johnston et al., 2003). Polyclonal antibodies included those specific for the proenzyme and cleaved forms of caspase-1 (1:1000, Upstate Biotechnology), IL-1β (1:1000, Cell Signaling Technology), and caspase-3 (1:1000, Cell Signaling Technology). Equal loading of each sample was confirmed by detection of the housekeeping gene, actin, by use of monoclonal antibodies obtained from Santa Cruz Biotechnology at a dilution of 1:3000. Horseradish peroxidase (HRP)-conjugated goat-anti-mouse and goat-anti-rabbit secondary antibodies were obtained from Jackson ImmunoResearch Laboratories.

RT-PCR

Necropsied tissue was ground under liquid nitrogen and passed through a QiaShredder (Qiagen) column to disrupt cells and connective tissue. Total cellular RNA was then isolated using a RNAeasy Mini Kit (Qiagen) and DNase treated for 30 min at 37ºC. cDNA was prepared using Superscript II RT (Invitrogen) and amplified with primers specific for rabbit IL-1β, IL-6, or MCP-1. Loading of equal amounts of template cDNA was assessed by amplification of GAPDH. Amplification of DNase-treated RNA obtained from each sample prior to reverse transcription served as controls to ensure the lack of contaminating DNA. PCR products were separated by agarose gel electrophoresis and visualized by staining with ethidium bromide.

Detection of Caspase-1 Activity and Cytokine Processing

Differentiated THP-1 cells were mock-infected or infected with wt or KO virus at an moi = 5, and cells and conditioned media (CM) were harvested at various time points PI. Activation of caspase-1 and subsequent processing of IL-1β and IL-18 was assessed by Western blot detection of the cleaved isoforms of each protein in cell lysates. Secreted IL-1β and IL-18 was detected in CM with quantitative human IL-1β and IL-18 sandwich ELISA Kits (R&D Systems) according to manufacturer's instructions. Levels of IL-1β and IL-18 in triplicate samples were quantified by referencing a standard curve generated

in parallel and expressed as pg cytokine/ml of CM. Caspase-1 activity was quantified using a colorimetric assay based on spectrophotometric detection of caspase-1 cleavage of the chromophore *p*-nitroaniline (*p*NA) from substrate containing the YVAD recognition site (Calbiochem). Mean values of triplicate samples (corrected for background) were expressed relative to untreated controls. Activation of caspase-1 and cytokine processing in response to exogenous stimuli was similarly assessed in cells that were mock infected or infected with wt or KO virus and cells that were transiently transfected with plasmid encoding full-length or truncated M13L. Stimuli included treatment with lipopolysaccharide (LPS, 600 μg, Sigma) for 1 hr or mechanical disruption of membrane integrity. To disrupt membrane integrity, cells were harvested in cold PBS, incubated for 15 min on ice in hypotonic buffer, and then passaged repeatedly through a 22 gauge needle.

Bioinformatic Analyses

The M13L sequence (accession number AF170726) was used as initial query in a BLASTp (Altschul et al., 1997) search of the public domain database to identify similarity to other proteins. A construction of multiple alignments with various PYD-containing proteins was carried out using the CLUSTAL W Multiple Sequence Alignment software (Thompson et al., 1994). Cell sorting predictions for M13L-PYD was carried out using PSORT II (Nakai and Horton, 1999), which determines the likelihood of the presence of a signal peptide and subcellular localization. The protein domain search tool Prosite (Appel et al., 1994) was used to identify putative patterns, profiles, and/or motifs present within the M13L amino acid sequence.

Acknowledgments

This work was supported by grants from the Canadian Institutes for Health Research (CIHR). G.M. holds a Canada Research Chair in Molecular Virology. J.B.J. held a CIHR Fellowship during completion of this work. We thank J. Reed for valuable reagents and helpful comments on this manuscript. We would like to dedicate this work to the memory of Frederique Messud-Petit.

Received: October 15, 2004
Revised: September 23, 2005
Accepted: October 7, 2005
Published: December 13, 2005

References

Afonso, C.L., Tulman, E.R., Lu, Z., Zsak, L., Osorio, F.A., Balinsky, C., Kutish, G.F., and Rock, D.L. (2002). The genome of swinepox virus. J. Virol. *76*, 783–790.

Akita, K., Ohtsuki, T., Nukada, Y., Tanimoto, T., Namba, M., Okura, T., Takakura-Yamamoto, R., Torigoe, K., Gu, Y., Su, M.S., et al. (1997). Involvement of caspase-1 and caspase-3 in the production and processing of mature human interleukin 18 in monocytic THP.1 cells. J. Biol. Chem. *272*, 26595–26603.

Altschul, S.F., Madden, T.L., Schaffer, A.A., Zhang, J., Zhang, Z., Miller, W., and Lipman, D.J. (1997). Gapped BLAST and PSI-BLAST: a new generation of protein database search programs. Nucleic Acids Res. *25*, 3389–3402.

Appel, R.D., Bairoch, A., and Hochstrasser, D.F. (1994). A new generation of information retrieval tools for biologists: the example of the ExPASy WWW server. Trends Biochem. Sci. *19*, 258–260.

Asefa, B., Klarmann, K.D., Copeland, N.G., Gilbert, D.J., Jenkins, N.A., and Keller, J.R. (2004). The interferon-inducible p200 family of proteins: a perspective on their roles in cell cycle regulation and differentiation. Blood Cells Mol. Dis. *32*, 155–167.

Barrett, J.W., Cao, J.X., Hota-Mitchell, S., and McFadden, G. (2001). Immunomodulatory proteins of myxoma virus. Semin. Immunol. *13*, 73–84.

Barry, M., and McFadden, G. (1997). Virus encoded cytokines and cytokine receptors. Parasitology *115* (*Suppl*), S89–S100.

Bertin, J., and DiStefano, P.S. (2000). The PYRIN domain: a novel motif found in apoptosis and inflammation proteins. Cell Death Differ. *7*, 1273–1274.

Calderara, S., Xiang, Y., and Moss, B. (2001). Orthopoxvirus IL-18 binding proteins: affinities and antagonist activities. Virology *279*, 22–26.

Cameron, C., Hota-Mitchell, S., Chen, L., Barrett, J., Cao, J.X., Macaulay, C., Willer, D., Evans, D., and McFadden, G. (1999). The complete DNA sequence of myxoma virus. Virology *264*, 298–318.

Centola, M., Aksentijevich, I., and Kastner, D.L. (1998). The hereditary periodic fever syndromes: molecular analysis of a new family of inflammatory diseases. Hum. Mol. Genet. *7*, 1581–1588.

Chen, X., Bykhovskaya, Y., Tidow, N., Hamon, M., Bercovitz, Z., Spirina, O., and Fischel-Ghodsian, N. (2000). The familial mediterranean fever protein interacts and colocalizes with a putative Golgi transporter. Proc. Soc. Exp. Biol. Med. *224*, 32–40.

Everett, H., and McFadden, G. (1999). Apoptosis: an innate immune response to virus infection. Trends Microbiol. *7*, 160–165.

Fairbrother, W.J., Gordon, N.C., Humke, E.W., O'Rourke, K.M., Starovasnik, M.A., Yin, J.P., and Dixit, V.M. (2001). The PYRIN domain: a member of the death domain-fold superfamily. Protein Sci. *10*, 1911–1918.

Fenner, F., and Ratcliffe, F. (1965). Myxomatosis (Cambridge, UK: Cambridge University Press).

Gubser, C., Hue, S., Kellam, P., and Smith, G.L. (2004). Poxvirus genomes: a phylogenetic analysis. J. Gen. Virol. *85*, 105–117.

Gumucio, D.L., Diaz, A., Schaner, P., Richards, N., Babcock, C., Schaller, M., and Cesena, T. (2002). Fire and ICE: the role of pyrin domain-containing proteins in inflammation and apoptosis. Clin. Exp. Rheumatol. *20*, S45–S53.

Hoffman, H.M., Mueller, J.L., Broide, D.H., Wanderer, A.A., and Kolodner, R.D. (2001). Mutation of a new gene encoding a putative pyrin-like protein causes familial cold autoinflammatory syndrome and Muckle-Wells syndrome. Nat. Genet. *29*, 301–305.

Hull, K.M., Shoham, N., Chae, J.J., Aksentijevich, I., and Kastner, D.L. (2003). The expanding spectrum of systemic autoinflammatory disorders and their rheumatic manifestations. Curr. Opin. Rheumatol. *15*, 61–69.

Johnston, J., and Power, C. (1999). Productive infection of human peripheral blood mononuclear cells by feline immunodeficiency virus: implications for vector development. J. Virol. *73*, 2491–2498.

Johnston, J.B., Barrett, J.W., Chang, W., Chung, C.S., Zeng, W., Masters, J., Mann, M., Wang, F., Cao, J., and McFadden, G. (2003). Role of the serine-threonine kinase PAK-1 in myxoma virus replication. J. Virol. *77*, 5877–5888.

Johnston, J.B., Nazarian, S.H., Natale, R., and McFadden, G. (2005). Myxoma virus infection of primary human fibroblasts varies with cellular age and is regulated by host interferon responses. Virology *332*, 235–248.

Kinne, R.W., Brauer, R., Stuhlmuller, B., Palombo-Kinne, E., and Burmester, G.R. (2000). Macrophages in rheumatoid arthritis. Arthritis Res. *2*, 189–202.

Lee, H.J., Essani, K., and Smith, G.L. (2001). The genome sequence of Yaba-like disease virus, a yatapoxvirus. Virology *281*, 170–192.

Lucas, A., and McFadden, G. (2004). Secreted immunomodulatory viral proteins as novel biotheraputics. J. Immunol. *173*, 4765–4774.

Mansfield, E., Chae, J.J., Komarow, H.D., Brotz, T.M., Frucht, D.M., Aksentijevich, I., and Kastner, D.L. (2001). The familial Mediterranean fever protein, pyrin, associates with microtubules and colocalizes with actin filaments. Blood *98*, 851–859.

Martinon, F., Burns, K., and Tschopp, J. (2002). The inflammasome: a molecular platform triggering activation of inflammatory caspases and processing of proIL-beta. Mol. Cell *10*, 417–426.

Masumoto, J., Taniguchi, S., Ayukawa, K., Sarvotham, H., Kishino, T., Niikawa, N., Hidaka, E., Katsuyama, T., Higuchi, T., and Sagara, J. (1999). ASC, a novel 22-kDa protein, aggregates during apoptosis of human promyelocytic leukemia HL-60 cells. J. Biol. Chem. *274*, 33835–33838.

Masumoto, J., Taniguchi, S., Nakayama, J., Shiohara, M., Hidaka, E., Katsuyama, T., Murase, S., and Sagara, J. (2001). Expression of apoptosis-associated speck-like protein containing a caspase recruitment domain, a pyrin N-terminal homology domain-containing

protein, in normal human tissues. J. Histochem. Cytochem. *49*, 1269–1275.

McDermott, M.F., and Aksentijevich, I. (2002). The autoinflammatory syndromes. Curr. Opin. Allergy Clin. Immunol. *2*, 511–516.

McLysaght, A., Baldi, P.F., and Gaut, B.S. (2003). Extensive gene gain associated with adaptive evolution of poxviruses. Proc. Natl. Acad. Sci. USA *100*, 15655–15660.

Messud-Petit, F., Gelfi, J., Delverdier, M., Amardeilh, M.F., Py, R., Sutter, G., and Bertagnoli, S. (1998). Serp2, an inhibitor of the interleukin-1beta-converting enzyme, is critical in the pathobiology of myxoma virus. J. Virol. *72*, 7830–7839.

Minagar, A., Shapshak, P., Fujimura, R., Ownby, R., Heyes, M., and Eisdorfer, C. (2002). The role of macrophage/microglia and astrocytes in the pathogenesis of three neurologic disorders: HIV-associated dementia, Alzheimer disease, and multiple sclerosis. J. Neurol. Sci. *202*, 13–23.

Nakai, K., and Horton, P. (1999). PSORT: a program for detecting sorting signals in proteins and predicting their subcellular localization. Trends Biochem. Sci. *24*, 34–36.

Opgenorth, A., Graham, K., Nation, N., Strayer, D., and McFadden, G. (1992). Deletion analysis of two tandemly arranged virulence genes in myxoma virus, M11L and myxoma growth factor. J. Virol. *66*, 4720–4731.

Reed, J.C., Doctor, K., Rojas, A., Zapata, J.M., Stehlik, C., Fiorentino, L., Damiano, J., Roth, W., Matsuzawa, S., Newman, R., et al. (2003). Comparative analysis of apoptosis and inflammation genes of mice and humans. Genome Res. *13*, 1376–1388.

Richards, N., Schaner, P., Diaz, A., Stuckey, J., Shelden, E., Wadhwa, A., and Gumucio, D.L. (2001). Interaction between pyrin and the apoptotic speck protein (ASC) modulates ASC-induced apoptosis. J. Biol. Chem. *276*, 39320–39329.

Seet, B.T., Johnston, J.B., Brunetti, C.R., Barrett, J.W., Everett, H., Cameron, C., Sypula, J., Nazarian, S.H., Lucas, A., and McFadden, G. (2003). Poxviruses and immune evasion. Annu. Rev. Immunol. *21*, 377–423.

Srinivasula, S.M., Poyet, J.L., Razmara, M., Datta, P., Zhang, Z., and Alnemri, E.S. (2002). The PYRIN-CARD protein ASC is an activating adaptor for caspase-1. J. Biol. Chem. *277*, 21119–21122.

Stehlik, C., and Reed, J.C. (2004). The PYRIN connection: novel players in innate immunity and inflammation. J. Exp. Med. *200*, 551–558.

Stehlik, C., Fiorentino, L., Dorfleutner, A., Bruey, J.M., Ariza, E.M., Sagara, J., and Reed, J.C. (2002). The PAAD/PYRIN-family protein ASC is a dual regulator of a conserved step in nuclear factor kappaB activation pathways. J. Exp. Med. *196*, 1605–1615.

Stehlik, C., Krajewska, M., Welsh, K., Krajewski, S., Godzik, A., and Reed, J.C. (2003). The PAAD/PYRIN-only protein POP1/ASC2 is a modulator of ASC-mediated nuclear-factor-kappa B and procaspase-1 regulation. Biochem. J. *373*, 101–113.

Thompson, J.D., Higgins, D.G., and Gibson, T.J. (1994). CLUSTAL W: improving the sensitivity of progressive multiple sequence alignment through sequence weighting, position-specific gap penalties and weight matrix choice. Nucleic Acids Res. *22*, 4673–4680.

Tulman, E.R., Afonso, C.L., Lu, Z., Zsak, L., Kutish, G.F., and Rock, D.L. (2001). Genome of lumpy skin disease virus. J. Virol. *75*, 7122–7130.

Tulman, E.R., Afonso, C.L., Lu, Z., Zsak, L., Sur, J.H., Sandybaev, N.T., Kerembekova, U.Z., Zaitsev, V.L., Kutish, G.F., and Rock, D.L. (2002). The genomes of sheeppox and goatpox viruses. J. Virol. *76*, 6054–6061.

Wang, G., Barrett, J.W., Nazarian, S.H., Everett, H., Gao, X., Bleackley, C., Colwill, K., Moran, M.F., and McFadden, G. (2004). Myxoma virus M11L prevents apoptosis through constitutive interaction with Bak. J. Virol. *78*, 7097–7111.

Xiang, Y., and Moss, B. (2003). Molluscum contagiosum virus interleukin-18 (IL-18) binding protein is secreted as a full-length form that binds cell surface glycosaminoglycans through the C-terminal tail and a furin-cleaved form with only the IL-18 binding domain. J. Virol. *77*, 2623–2630.

Yu, J.W., Wu, J., Zhang, Z., Datta, P., Ibrahimi, I., Taniguchi, S., Sagara, J., Fernandes-Alnemri, T., and Alnemri, E.S. (2005). Cryopyrin and pyrin activate caspase-1, but not NF-kappaB, via ASC oligomerization. Cell Death Differ., in press.